A detailed aircraft tyre finite element model for hard landing safety assessment

Hua Guo, Christophe Bastien, Mike V. Blundell, Gary Wood

Coventry University, Dunlop Aircraft Tyres Limited

1   Abstract

Tyres have an important role in landing gear systems upon aircraft landing and taxing on the ground. The performances of an aircraft tyre under varied load conditions are vital requirements for aircraft safety certification.

This paper describes the development of a detailed finite element (FE) model of an aircraft test tyre in order to investigate its performance and assess its safety criteria. The work follows the findings from previous researches [1] [2] [3] [4] and focuses on the aircraft tyre safety assessment under various loading scenarios that were not yet studied.

Initially, tyre inflation and static load simulations have been analyzed based on a full-scaled 3D detail LS-Dyna® FE model, replicating the actual geometry and the correlated material properties from industrial experimental data.

The dynamic simulations that aim to duplicate tyre load upon aircraft landing scenarios have also been analyzed. Following the comments from aircraft tyre industrial data and guidelines[5] [6], the dynamic simulations have covered the tyre loading scenario from on-road taxing, normal (soft) landing, hard landing to crash landing under different aircraft landing weights. The stresses on tyre/wheel contact areas and on bead cords have been chosen as the safety criteria. The simulation results, analysis and comments have been discussed in great details.

The modelling and simulations described in this paper aim to demonstrate the effective use of FE models for aircraft safety assessment, by studying the criteria of the tyre for load cases corresponding with testing and operational scenarios.

The development of such predictive model would allow the manufacturers to assess tyre availability during the design process, and also add to the general drive towards the use of more virtual prototypes in an area traditionally reliant on experimental testing.

Key Words: Aircraft tyre, Predictive model, Safety assessment, FEA, LS-Dyna, Hyperelastic rubber

2   Introduction

Aircraft tyres play an important role in a landing gear system. They are critical for aircraft safety and performance upon landing and taxing on the ground. The performances of a tyre under varied load conditions are vital requirements for aircraft safety certification.

In this paper, a detailed finite element model has been constructed in order to investigate the tyre performance and its safety criteria. The work follows the finding from previous research [1] [2] [3] and focuses on the tyre safety assessment under various loading scenarios that were not yet studied. It aims to demonstrate the effective use of FE models for aircraft safety assessment, by studying the criteria of the tyre for load cases corresponding with testing and operational scenarios.

By analyzing the specific aircraft tyre and wheel interaction model for different load cases, crucial data such as the stress distribution around tyre and wheel rim for a particular design can also be obtained.

The proposed paper will introduce the FE modelling of an actual aircraft testing tyre, the review of material characterisation [4] and the correlation undertaken, the reliability of the full 3D tyre model against the inflation load case, the current finding on the correlation of the aircraft tyre static load test, the predictive safety assessment under various dynamic loading scenarios and the outlook and opportunities to complete such a tool to improve aviation safety.

3   Process of Modelling Aircraft Tyre

The proposed paper is based on a dual bead radial ply H41x16.0R20 testing tyre from the cooperation company, Dunlop Aircraft Tyres Limited (DATL).

3.1   Parts and materials of tyre

Typical aircraft radial tyres contain one bead cord [7], creating a small bead chafer area contacted with the wheel rim. Under a certain load condition, a small chafer area will result in large contact pressure. However, the chosen H41x16.0R20 test tyre has a double bead cord design (Fig. 1), which enlarged the chafer area compared to the single bead cord design.

The FE modelling of this specific tyre/wheel interaction is supposed to provide detailed results around the contact area which could be utilized in further industrial product development.

The structure definition for the target tyre includes:
- Cable beads: Bead Code, Bead Wrapping
- Fabric: Chafer, 1st to 4th Plies, Bias Breakers, 0 Deg. Belts, Inner Tread Fabric
- Rubber Compounds: Chafer, Inner Liner, Apex, Clinch, Insulations, Sidewall, Breakers Cushion and Strips, Sub Tread, Tread [8]

3.2   Finite element model of tyre

Several simplifications in the FE model have been made: clinch and sidewall are considered as the same part, Chafer and Apex are categorised as the same part although they are separated in the model.
The major construction parts used in the tyre FE model include:
- Tread: The component that contactes with the road and provides traction properties.
- Belts: This part is composed of fabrics that encased in rubber, providing puncture resistance.
- Sidewall and Apex: They run from the rim of the wheel to the tread, providing lateral stability and resistance to the vertical compression of the tyre.
- Bead: It locks the tyre onto the wheel rim, stops the sidewall separating from the rim and therefore lose tyre air pressure.
- Plies: They run perpendicular to the direction of the tread and belts, serve as the main reinforcement materials of the tyre.

In the model, tread, sidewall, apex and bead are modelled with solid elements, various layers. Both the plies and belts are modelled with a combination of beam and solid elements. It allows the different materials to behave independently. Mentioned by Reid [1], this method allows the tyre to get lateral stability from the beams, which are only tied together in the radial direction by the sidewall rubber.

As shown in Fig. 1, the details of the target tyre are provided by DATL. A 2-D model of the tyre cross-section was built according to its realy geometry. In the 2D model, shell elements in size 5mm are temporarily used to represent its major components: tread (purple color), belts (dark blue), sidewall (yellow), apex (light blue), bead (red) and plies (green).
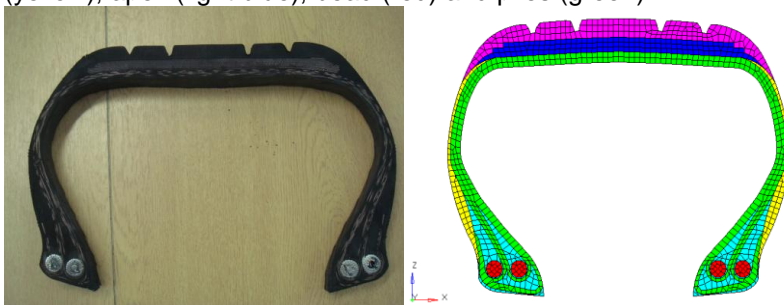

Fig. 1: Comparison between H41x16.0R20 tyre cross-section and FE model [8]

The apporach of developing 3D tyre model is to rotate 2D cross-section model 360 degrees by 10 degrees per step. 3D solid elements are therefore generated by rotating the shell elements. The components of the tyre are individually signed with different material properties, which will be discussed in details afterwards.
The beam elements are then generated through extracting lines on solid elements' boundaries. It's worth mention that the plies' fabirc (yellow beams in Fig. 2) run perpendicular to the direction of the belts' and inner tread fabrics (red and green beams in Fig. 2).

As a summary, in the 3D tyre model, solid elements are used to represent rubber. The beam elements used to represent fabric are merged with the solid elements.

Total element numbers for the tyre model are: 40140 solid elements and 18972 beam elements. Initially, the simulation time step was set to be 4.43154E-7s in LS-Dyna, which resulted in a 0% added mass at time step 0s. Referring to the simulation result *.otf file, time steps were controlled by the 100 smallest solid elements in the Apex part. Those elements are located around the contact area between the tyre and the wheel rim, and are needed to be small to duplicate the actual geometry.
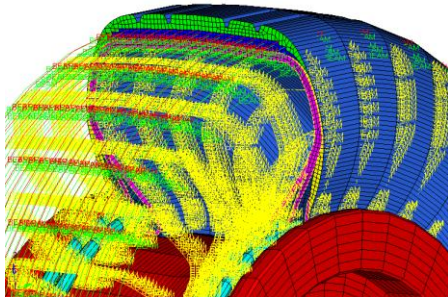

Fig. 2: 3D H41 Dual bead meshed tyre

The relationship between time step and percentage age added mass is shown in Table. 1. It is worth mentioning that a 2% added mass has been recognized as an industry standard criterion, beyond which LS-Dyna FE models are considered as not reliable because of added inertial effects. Therefore, FE models with 2 different simulation time steps have been processed. The results and comparison between them will be discussed in the following section.

Time Step (s)	Age added mass (%)
4.43E-07	0
5.07E-07	1
5.31E-07	2

Table. 1: Time Steps for specific percentage age added mass

4   Material Characterisation and correlation

It is noticed that rubber and fabric composite materials are the major components of an aircraft tyre. Their characterisation requires tests and correlation.

Rubber material usually has long chain molecules. [9] It presents a complicated mechanical behaviour that exceeds the linear elastic theory and contains large deformations, plastic and viscoelastic properties and stress softening [10] [11].

In general, rubber can be defined by a stored energy function as hyperelastic material. The coefficients in these functions should be determined by uniaxial, biaxial and shear test data. As highlighted in Ali's work [4], the essential problem is to determine the strain energy function for providing good fit with a number of sets of experimental data.

Yang [12] also emphasised the complexity when determining rubber materials' hyperelastic and viscoelastic characteristics. The researches regarding fitting and comparison of such models with experimental test data can also be seen in Markmann [13], and Ogden's [14] work. Other examples in tyre FE application using hyperelastic models have been published by a number of researchers, such as Shiraishi [15] and Zhang [16]. It can be concluded from the previous researches that the selection of an appropriate strain energy model is of significant importance to ensure that the FE simulation is able to replicate the response of the tyre accurately.

Take the rubber material DC001 for example, the correlated the material is used for the tread tyre component.

With its database, LS-Dyna has numerous material cards to represent rubber material models, including Mooney-Rivlin rubber, Frazer-Nash rubber, General Viscoelastic (Maxwell Model), Hyperelastic and Ogden Rubber (Yeoh model), Arruda Boyce Rubber and etc [17]. It is noticed that each material cards in LS-Dyna requires the setting of orders, coefficients, or relative experimental data of each individual energy function.

Regarding the fact that the actual material properties data are curves giving force versus actual change in the gauge length only from uniaxial tensile tests, (with sample size gauge length 25mm, width 4mm and thickness 2mm), [8] the Yeoh model, which represent as *MAT_77 hyperelastic rubber in LS-Dyna has been chosen.

To correlate the tyre tread rubber model DC001, a simulation has been processed using a 3rd order Yeoh model. The FE sample model, with regard to the actual sample size used for experimental tensile test in DATL has been built (25 mm in length, 4 mm in width and 2 mm in thickness). A prescribed displacement on the FE sample has been applied to simulate the uniaxial tensile. A cross-section has been set in the middle of the sample to collect the force vs. time curve from the simulation. The force vs. Displacement curves from simulation and experimental test for the rubber material DC001 are displayed in Fig. 3.
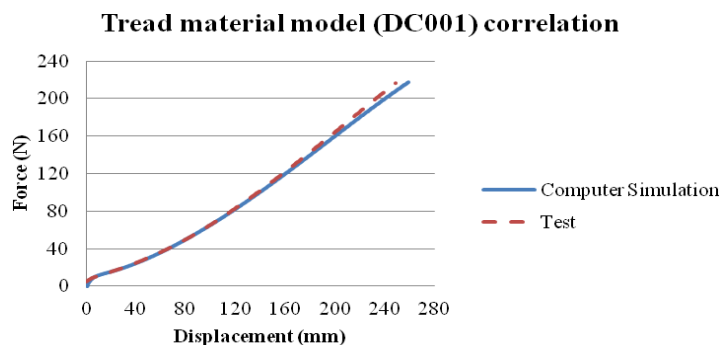

Fig. 3: Material correlation for tread rubber DC001

From Fig. 3, it can be concluded that the tread material model has been correlated with the test.

Following the same process, the correlations of the other rubber and fabric materials used in the H41 tyre model have been achieved. All material models have been validated through comparing LS-Dyna simulations to DATL test data.

As a conclusion, Table. 2 below shows all the details of the element types (section card in LS-Dyna), finite element formulation, material model (material card in LS-Dyna) that were used for the tyre finite element model respectively.

Part	Material Code	Poison's Ratio	Density kg/mm3	Young's modulus GPa	Element	Mat_Card
Tread	DC001	0.495	1.10e-6	N/A	Solid	MAT_77
Belt	DC005	0.495	1.10e-6	N/A	Solid	MAT_77
Sidewall	DC012	0.495	1.10e-6	N/A	Solid	MAT_77
Apex	DC003	0.495	1.10e-6	N/A	Solid	MAT_77
Plies	DC005	0.495	1.10e-6	N/A	Solid	MAT_77
Belt Fabric	DF021	0.28	7.86e-6	200	Beam	MAT_67
IT Fabric	DF014	0.28	1.39e-6	5	Beam	MAT_67
Ply Fabric	DF014	0.28	1.39e-6	5	Beam	MAT_67
Bead	N/A	0.28	7.86E-6	200	Solid	MAT_1

Table. 2: H41x16.0R20 Tyre Parts Material properties

MAT_77: Hyperelastic rubber
MAT_67: nonlinear elastic discrete beam
MAT_1: elastic

5   Simulation and validation under static load scenarios

In order to validate the FE tyre model, simulations duplicating aircraft tyre testing and operational scenarios have been designed and tested.

5.1   Setup of the Inflation scenario

In this scenario, the 3D FE tyre model was mounted to the corresponding wheel FE model, which is fully constrained at the bearing. The volume of the tyre was inflated from 0 to 187psi (equal to 1.289MPa, recommended by the tyre manufacturer). The tyre pressure can be modelled in different ways [3] [12] [16]. The chosen method is to apply the control volume option by using an LS-Dyna *AIRBAG command. The deformations of the tyre cross-section and the airbag pressure from simulation have been compared with the experimental data in order to validate the FE model, as will be explained in this section.

5.2   Setup of the Static load scenario

This scenario involves squashing the tyre against a rigid plane. To achieve this, the wheel is clamped, with the inflated tyre mounted on it. The vertical load is achieved by placing a rigid moving wall below the tyre and then prescribing an upward displacement towards the tyre. The actual simulation process is: first inflating the tyre, then pushing the rigid against the inflated tyre. The scenario in LS-Dyna is shown in Fig. 4. Forces on the wall, as well as the tyre deformation on the tyre/road contact interfaces are recorded in order to compare with the experimental test results from DATL.
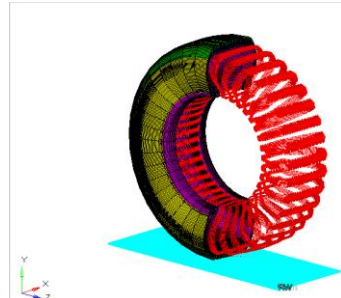

Fig. 4: Static load scenario in LS-Dyna

5.3   Results and comparison of both scenarios

5.3.1 Inflation

The deformations of the tyre cross-section have been selected to examine the reliability of the tyre FE model. Outlay of the tyre model after inflation, along with the points of measurements in LS-Dyna can be seen in Fig. 5.

The expected tyre cross-section widths, X deformation, outside diameter and Z/Y deformation have been listed in Table. 3 below. The relevant results provided by the LS-Dyna inflation simulation have also been listed.

Neglectable differences are between the experimental inflation test and the LS-Dyna simulation. Compare 0% age added mass simulation with the test data, the X deformation has an only 0.3mm difference at section width measure point. And the Y/Z deformation only has a 3.44% difference.

The outputs are showing that the pressure is applied as expected to the tyre as the tyre diameter is increasing due to the inflation loading. For Y deformation, inflation simulation have resulted in just a slight difference as shown in Table. 3.

		Section Width (mm)	X deform (mm)	Out diameter (mm)	Y/Z deform (mm)
DATL test		330.00	2.5	1034.00	20.35
LS-Dyna 0% added mass	Magnitude	329.4	2.2	1032.60	19.65
	Differ (%)	1.08%	12%	0.14%	3.44%
LS-Dyna 2% added mass	Magnitude	328.5	1.75	1032.70	19.70
	Differ (%)	1.35%	30%	0.13%	3.19%

Table. 3 Inflation test and simulation results

It is noticed that there is a 30% difference in X deformation from 2% added mass time step simulation. However, the actual magnitude difference is only 0.75mm out of 2.5mm. Regarding the small difference in actual section width (1.08% and 1.35%), that 30% difference is not considered as a fault. To prove this point, both 0% and 2% added mass simulations have been processed in static load scenario, and the outputs are compared in the following section to validate the reliability of the 2% added mass time step simulation.
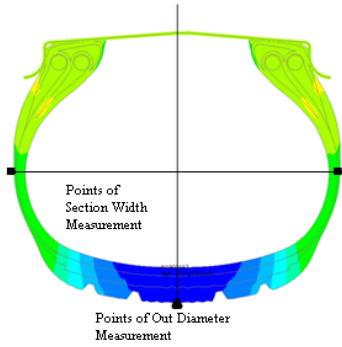
Fig. 5: Tyre cross-section before and after inflation, points of measurements

5.3.2   Static load

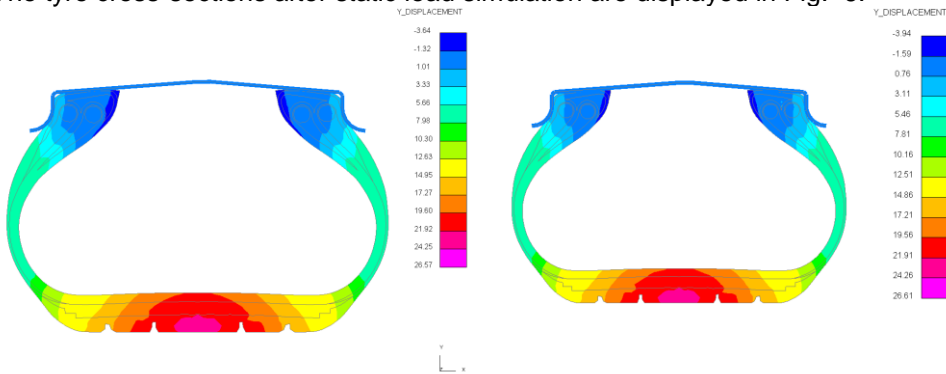The tyre cross-sections after static load simulation are displayed in Fig. 6.

Fig. 6: Tyre cross-sections after static load
(Y deform left: 0% added mass, right: 2% added mass)

It is worth mentioning that in static load scenario, the deformation of the tyre under both 0% and 2% added mass time steps are following the same trend as expected. The recorded Y deformations and X deformations are listed in Table. 4. The differences are neglectable, which indicates the reliability of the 2% added mass time step simulation.

Time Step (s)	Mass scaling	X deformation (mm)	Y deformation (mm)
4.43E-07	0% added mass	15.17	26.57
5.31E-07	2% added mass	15.15	26.61
Difference (%)		0.13%	0.15%

Table. 4 Static load scenario results

The load vs. force curve from the static load simulation has also been compared with DATL load vs. deflection result, which can be seen in Fig. 7. The results from DATL test and LS-Dyna simulation are very close, and the trends of two curves followed with each other as expected.
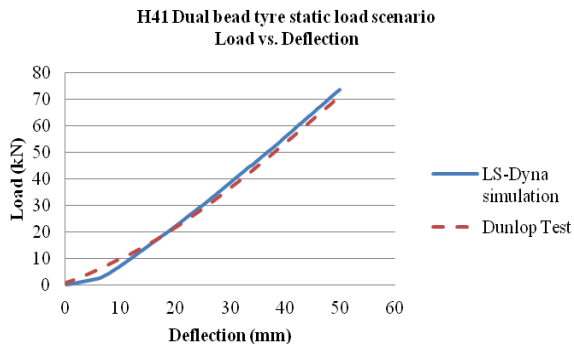

Fig. 7: Load vs. Deflection Dual Bead H41 tyre/wheel assembly under static load

6   Analysis and comparison between single bead and dual bead tyre

6.1   Single bead H41 dummy tyre model

To compare with H41 dual-bead tyre, a 3D single bead tyre FE model has also been developed. This 'Dummy' single bead tyre model has been generated basing on the actual dual bead tyre structure.
As shown in Fig. 8, single bead tyre has only one bead cord on each side and the number of the layers in body plies rubber and fabric compound has been reduced. The tyre/wheel rim contact area has also decreased, which leads to the structure change of the Apex part as well.
Apart from the parts mentioned above, the structures of Tread, Belt and side wall (including rubber and fabric) remain the same as the dual bead tyre. The materials used in single bead model are as the same as the ones correlated and used in dual bead tyre model.
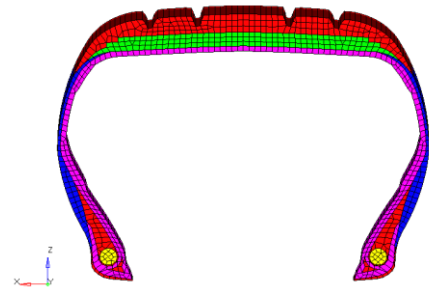

Fig. 8: 'Dummy' single bead H41 tyre cross-section

6.2   Tyre/wheel assembly model and simulations

The tyre/wheel assembly model has been developed for the tyre/wheel interaction analysis. It is noticed that the bolt pre-load will mainly affect the stress distribution around the bolt holes area. On the rim side, there's no significant stress contribution from the bolt pre-loads. Therefore, the structure of the assembled wheel hub has been simplified: the bolt hole strucutre has been ignored.
Both the dual bead and single bead 3D H41 FE tyre models have been mounted on the wheel hub, with the same simulation scenarios include inflation and static load as described in Chapter 5.1 and 5.2.
Additionally, dynamic simulations are designed to duplicate scenarios that the FE aircraft tyre falls and hits a rigid ground, carrying certain aircraft weights with various vertical landing speeds.
As shown in Fig. 9, the simulation duplicates a tyre drop on a rigid ground vertically from a certain height. The additional aircraft weight is achieved by assign *ELEMENT_MASS on the node at the centre of the tyre. *RBE3 elements are used to constrain wheel rim to the node. Landing speed is achieved by using *INITIAL_VELOCITY_GENERATION on the model. *CROSS_SECTIONS are also set up to collect the load on the beads.
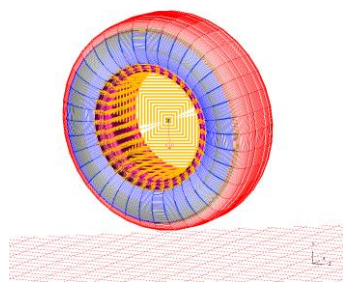

Fig. 9: Tyre and Rim constrains in LS-Dyna

6.3   Set up of vertical impact scenario

For the dynamic simulation, aircraft landing weight and vertical touch down speed have been defined in detail.
The wheel Weight is defined as 128.6kg from LS-Dyna calculation. Two different aircraft weight load cases are assumed and applied on tyre: empty weight 7400kg and Max landing weight approximate 11675kg. The assumption is based on that the actual size of the H41 testing wheel is close to the commercial aircraft tyres that are used on Boeing 737-200 as shown in Table. 5. [5]
Boeing 737-200 has 6 tyres (2 nose tyres, 4 main tyres) and its empty weight: 29600kg; max landing weight: 46700kg. [18] Assuming 4 tyres equally carry the aircraft weight upon landing, the mass on each tyre will be: 7400kg in empty weight and 11675kg in max landing weight.

	Aircraft Type	Main Tyre Code/Size
General Aviation/ Business Aircraft	Cessna 172, Skyhawk	6.00-6
	Dassault 10, Falcon	22x5.75-12
Commercial Aircraft	Douglas DC-4	15.50-20
	Boeing 737-200	H40x14.5-19

Table. 5: Aircraft tyre application and data [5]

Downward vertical velocity (vertical landing speed) is defined:
- 2 to 4 m/s normal landing
- 6 to 8 m/s hard landing
- Over 8m/s crash landing [19]

Considering the significance of landing speed change in crashworthiness certifications and analysis, the simulations have been processed with 0 m/s (free fall), 4m/s, 6m/s, 8m/s and 10m/s vertical landing speeds, separately.

6.4   Results and discussions

6.4.1 Inflation on tyre/wheel assembly model

The outlays from inflation simulation are as shown in the Fig. 10 below. The results for dual bead tyre/wheel are listed on the left side, and the single bead on the right.
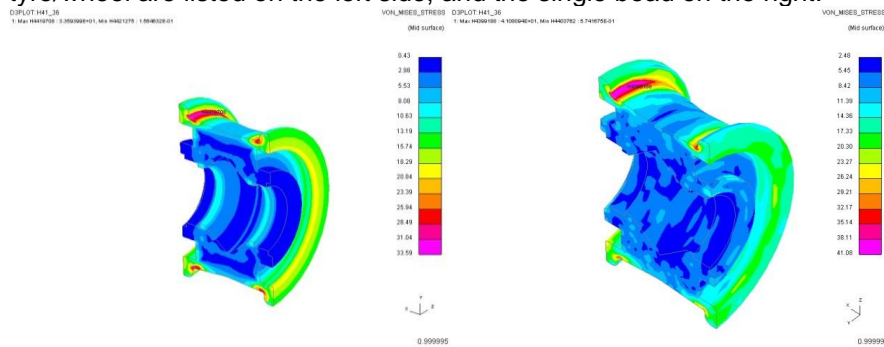

Fig. 10 Assembly Inflation, Von Mises Stress distribution on Hub
Left: Dual Bead Maximum value 33.59 MPa
Right: Single Bead Maximum value 41.08 Mpa

The simulation shows that due to tyre strucutre change, the interaction between tyre/wheel has been significantly affected. The Von Mises Stress value on the wheel hub with single bead tyre mounted, is 22% more than the dual bead tyre. The difference between single bead and dual bead model is intuitionistic: single bead tyre has a smaller sized bead and apex geometry, hence a smaller contact area which will result an increased stress.

6.4.2 Static load on tyre/wheel assembly model

The stresses on bead and apex boundaries from static load simulation have been shown in Fig. 11.
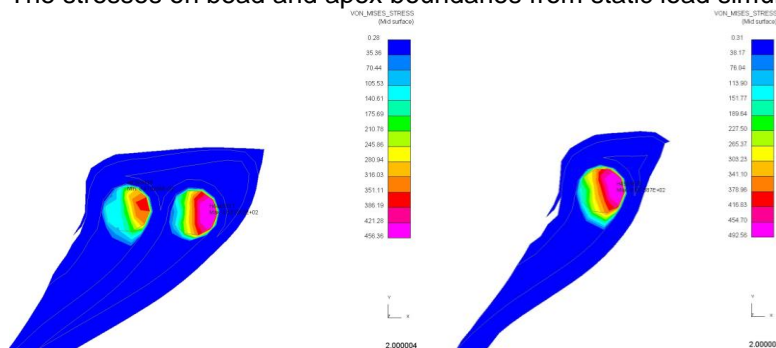

Fig. 11: Static load Von Mises Stress on Component Boundary
(Cross-section on the tyre/road contacted side)
Left: Dual bead Max 456.36 MPa,
Right: Single Bead model Max 492.56 MPa

The results from static load on assembly model follow the same trend as the inflation scenario. The stress distribution on component boundary differed due to tyre structure change. The bead and the part of apex that in contact with bead cord suffered 7% more stress in a single bead model.

6.4.3 Assembly model impact on rigid road under various speeds

Table-7 below shows the comparison between dual bead and single bead model under different vertical touch down speed.

Vertical speed (m/s)	Dual Bead model					Single Bead model				
Vertical speed (m/s)	0	4	6	8	10	0	4	6	8	10
Max Bead Force (kN)	40.51	42.43	45.42	67.76	73.57	46.76	48.97	57.67	74.34	85.46
Max Stress (MPa)	456.36	487.53	492.27	529.34	554.68	492.56	507.39	510.45	553.10	590.43

Table. 7: Max Force/Stress value comparison

In Fig. 12, a comparsion of the max stresses on beads with the yield strength (620MPa) and tensile strength (700MPa) of high-tensile steel [20] can be seen. The simulations are processed on both dual and single bead tyre models under various touch down speeds.
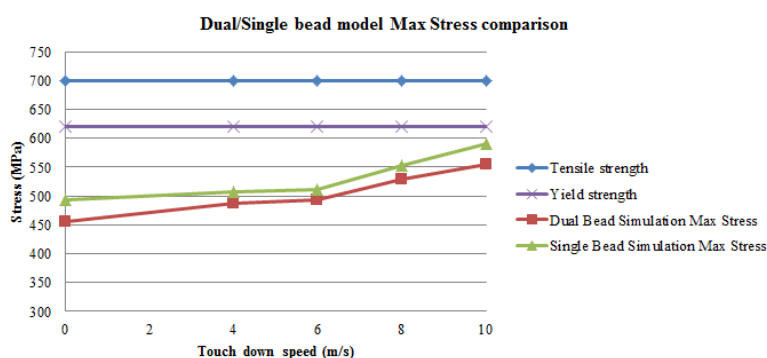

Fig. 12: Max Stress comparison between dual bead and single bead model

Comparing the dynamic simulation results between the dual and single bead models, it can be found that both the force and stress maximum value from a single bead model are higher than a dual bead model. It consists with the conclusion from inflation and static load scenarios. It is also noticed that the values increase with the rising touch down speeds, which follows the trend as expected. From Fig. 12, it can also be seen that for both models, the max stresses are within the range of material's yield and tensile strength. The dynamic simulations have indicated that the materials are in safe range for both the dual and single bead designs even under a high touch down speed. (10m/s, crash landing)

7 Conclusions

The present research has introduced a detailed approach of developing FE models for aircraft tyre.
The proposed model is suitable to run with a time step up to 5.31E-07s, giving a mass scaling of 2% at the beginning of the simulation, which is compatible to industry standards.
The initial investigations have covered tyre inflation and static load scenarios. Comparing with experimental test data, the results have indicated a reliable FE aircraft tyre/wheel interaction modelling approach. Tyre/wheel interaction has also been analyzed and compared between dual and single bead tyre model.
The study has also considered the effect of the aircraft landing phase on the tyre, by modelling and predicting a single tyre hitting the ground. An initial safety assessment, focusing on material properties (yield and tensile strength) of the test tyres has been achieved. The current work has demonstrated the effective use of finite element models as a predictive engineering tool. A further assessment can also be approached by investigating the tyre application criteria, such as tyre deflection rate and rated load. [21]
On-going research will investigate a combined 'free-falling' tyre with a rotation motion against a rigid road, duplicating the actual aircraft tyre working condition. The tests will aim to replicate tyre deformations, motions, rebound energy and validate this FE model in more complex dynamic events.

8   Acknowledgement

The author would like to thank: Dr. Wei Ding who was the head of R&D department in Dunlop Aircraft Tyre Limited for his technique support.

9   Summary

- A full-scaled LS-Dyna finite element aircraft tyre model has been developed.
- Rubber and fabric material properties have been characterised and correlated.
- The FE tyre model has been validated by comparing static simulations with tests.
- Both dual and single bead models have been developed to analyzed the tyre/wheel interaction.
- Dynamic simulations have been analyzed to achieve landing safety assessment.

10   Literature

[1] Reid, J. D. et al, "Detailed tyre modelling for crash applications", ICRASH 2006, Athens Greece, 4th-7th July 2006

[2] Hall, W. et al, "Tire Modelling Methodology with the Explicit Finite Element Code LS-DYNA", Tire Science and Technology, Vol. 32, No. 4, pp. 236-261, 2004

[3] Hall, W. et al, "Finite element simulation of a rolling automotive tyre to understand its transient macroscopic behaviour", Part D: Journal of Automotive Engineering, 2004 218:1393, 2004

[4] Ali, A. et al, "A review of Constitutive Models for Rubber-like materials", American J. of Engineering and Applied science, 2010

[5] Michelin, "Michelin Aircraft tyre engineering Data", http://www.airmichelin.com/generalcontent.aspx?id=219 site accessed on 21st Sep 2012

[6] Goodyear, "Goodyear Aircraft Tyre Data Book", http://www.goodyearaviation.com/resources/pdf/db_airdatabook.pdf site accessed on 21st Sep 2012

[7] Tanner, J. et al, "Mechanical Properties of Radial-Ply Aircraft Tires", SAE 2005-01-3438, USA, SAE International, 2005.

[8] Dunlop Aircraft Tyres Limited, "H41x16.0R20 tyre documents", 2010

[9] Smith, L.P., "The Language of Rubber: An introduction to the specification and testing of elastomers". London: Butterworth-Heinemann Ltd, ISBN: 10:0750614137, 1993, pp: 257

[10] Changon, G. et al, "A comparison of the Hart-Smith model with Arruda-Boyce and gent formulations for rubber elasticity". Rubber Chem. Technol., 2004, 77:724-735. http://cat.inist.fr/?aModele=afficheN&cpsidt=16233017,site accessed on 20th Sep 2012

[11] Naser, B. et al, "Durability Simulations of Elastomeric Structures". In: Constitutive Models for Rubber IV, Austrell, P.E. and L. Kari (Eds.). AA Balkema Publishers, UK., ISBN:10:0415383463, 2005, pp: 45-50

[12] Yang, X. et al, "Materials Testing for Finite Element Tire Model", SAE International, 2010-01-0418, Published on 04/12/2010

[13] Markmann, G. and Verron, E. "Comparison of hyperelastic models for rubber-like materials", Rubber Chem. Technol. 2006

[14] Ogden, R.W. et al, "Fitting hyperelastic models to experimental data", Comput. Mech., 2004, 34: 484-502

[15] Shiraishi, M. et al, "Developing FE-tyre model library for durability and crash simulations", 7th European Ls-Dyna Users' Conference, 2009

[16] Zhang, X. et al, "Finite Element Tyre Model Parameters for Road Load Predictions", SAE international No.05M-242, 2004

[17] LS-Dyna™, "Keyword manual, version 971", 2007

[18] Airline inform, "Boeing 737-200", http://www.airlines-inform.com/commercial-aircraft/Boeing-737-200.html site accessed on 20th Oct 2012

[19] RestArts, "Critical situations in take-off or landing flight phase", http://www.fp7-restarts.eu/index.php/home/root/state-of-the-art/objectives/2012-02-15-11-58-37/75-book-video/how-a-plane-can-fly-assuring-safety/138-5-critical-situations-in-take-off-or-landing-flight-phase site accessed on 10th Dec 2012

[20] Granta Design Limited, CES EduPack 2012 version 11.9.9, Material Properties of High-tensile steel, accessed on 21st Dec 2012 from EC, Coventry University

[21] Goodyear, "Aircraft tyre care and maintenance" http://www.goodyearaviation.com/resources/pdf/aircraftmanual.pdf site accessed on 10th Dec 2010